A 3.4-GHz Double Patch Pike-Shape Antenna for Wireless Applications

Constantinos T. Angelis*, Eirini Tsiakalou, and Christos Koliopanos

Department of Informatics and Telecommunications,
Technological Educational Institute of Epirus, Arta, Greece
kangelis@teiep.gr, {etsiak,xkoliopanos}@teleinfom.teiep.gr

Abstract. The goal of this paper is to investigate the performance of double patch printed antenna for wireless applications. The antenna is characterized in terms of impedance bandwidth, gain and radiation patterns through simulations. Simulations present satisfactory radiation pattern. The proposed antenna has the advantage of compact size, which makes it attractive for mobile devices.

Index Terms: Ultra-Wideband, Printed antennas, WiMax.

1 Introduction

During the last years there has been tremendous growth in wireless communication technology, especially for the IEEE 802.16 and IEEE 802.20 Worldwide Interoperability for Microwave Access (WiMAX) standards. Many researchers work in designing single, dual and tri-band antennas for WLAN/WiMAX applications [1-7]. The proposed antenna has the advantage of compact size, which makes it attractive for mobile devices.

The remaining of this paper is organized as follows: Section 2 describes the basic antenna design; Section 3 presents the simulation results and extensive numerical and simulation evidence of the proposed antenna; and the conclusions are given in Section 4.

2 Antenna Design

The proposed antenna is etched on a substrate of thickness 1.52 mm and dielectric constant of 3.38. The substrate has a compact dimension of 30 x 40mm^2. Fig. 2 shows the structure of the proposed antenna. The antenna consists of a single layer, which is the radiating layer as the ground plane of the antenna is located on the same side of the CPW-feed and radiating portion. The antenna is simulated using the parameters given in Table 1. The complete 3D structure is presented in Fig. 2 where it is possible to observe the patch of the antenna and its feeding plate.

Fig. 1 shows a pike-shape patch that is excited by a microstrip line through EM coupling.

* Member IEEE, ICST, EuMA.

C.T. Angelis, D. Fotiadis, and A.T. Tzallas (Eds.): AMBI-SYS 2013, LNICST 118, pp. 104–112, 2013.

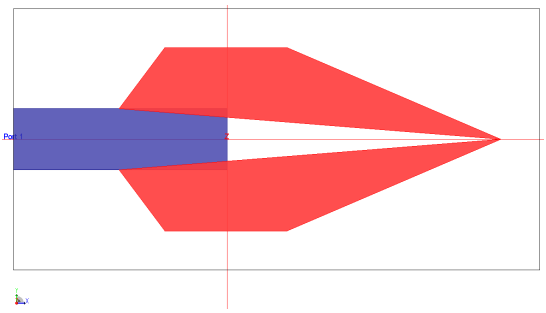

Fig. 1. Two dimensional structure of the proposed pike-shape double patch antenna

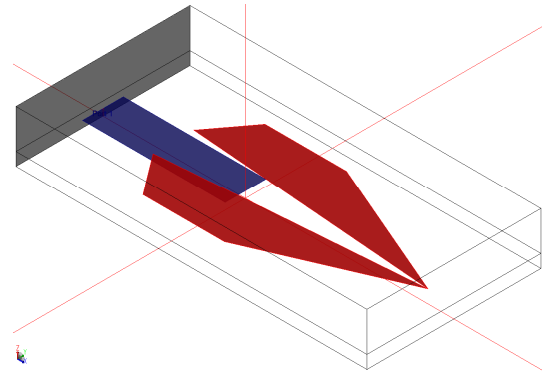

Fig. 2. Three dimensional structure of the proposed pike-shape double patch antenna

3 Results and Discussion

To verify our design approach and in parallel the effectiveness and feasibility of the proposed design we used simulation with ADS software. Simulations performed with Method of Moments and Finite Element Method. The Method of Moments was used to find the resonant frequency of the proposed antenna. A moment method analysis of planar circuits in a layered medium is developed. The Green's functions of a two-layer grounded medium are used in order to take into account the effect of the surface

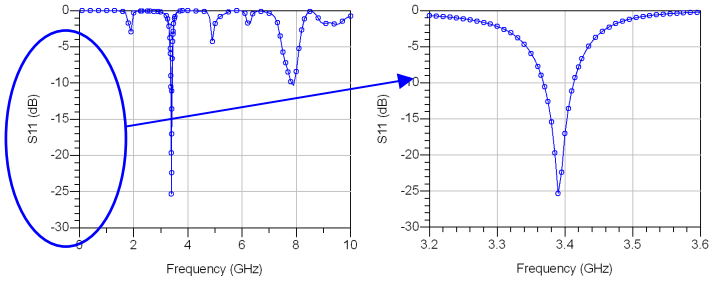

Fig. 3. Simulated reflection coefficient versus frequency

wave, coupling, and radiation. Interpolation techniques are used to increase computational efficiency. The embedded conductors are modeled with triangular patches. Results for several configurations, including direct and proximity coupled radiators, are in good agreement with measurements and other calculations. Fig. 3 shows the simulated Return loss. The current is predominantly excited at the pike-shape patch. The Bandwidth of the proposed antenna is 250MHz.

A. 2-D Far Field Calculations at 3.4 GHz

Two dimensional (2-D) far field calculations were performed with the Finite Element Method.

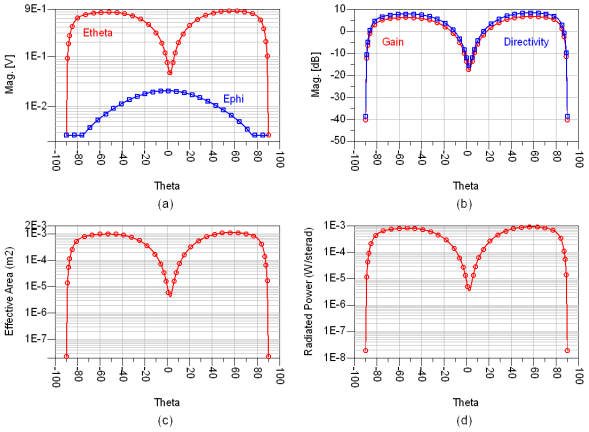

Fig. 4. (a) Absolute field strength (in volts) of the theta and phi electric far-field components, (b) Gain, Directivity, (c) Effective area (in m2), (d) Radiation intensity (in Watts/steradian), in the XZ-plane

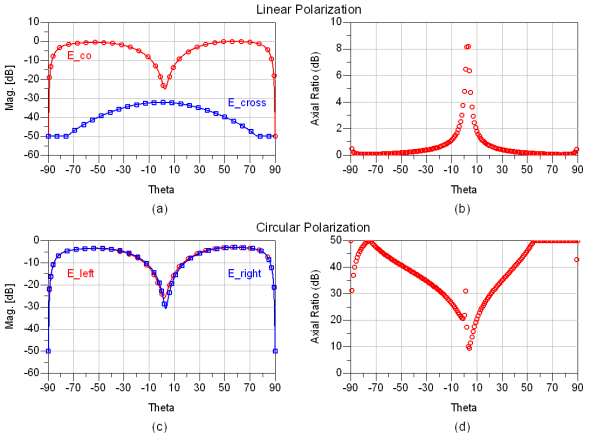

Fig. 5. (a) Normalized field strength of co and cross polarized electric far-field components, (b) Axial ratio, derived from left-hand and right-hand circular polarized far-field components, (c) Normalized field strength of respectively left-hand and right-hand circular polarized electric far-field component, (d) Linear polarization axial ratio, derived from co and cross polarized far-field components

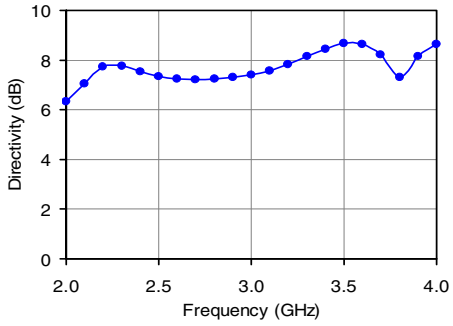

(a)

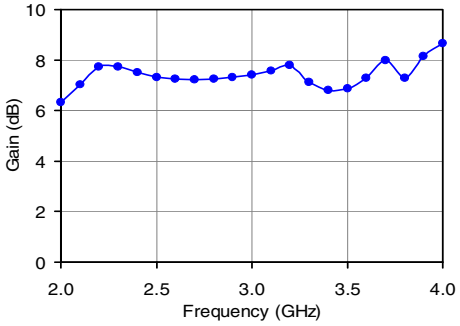

(b)

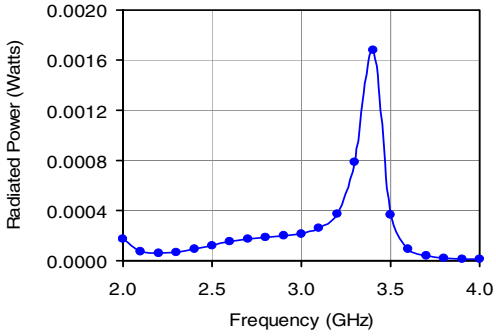

(c)

Fig. 6. (a) Directivity, (b) Gain, (c) Radiated Power and (d) % Injected Power versus frequency

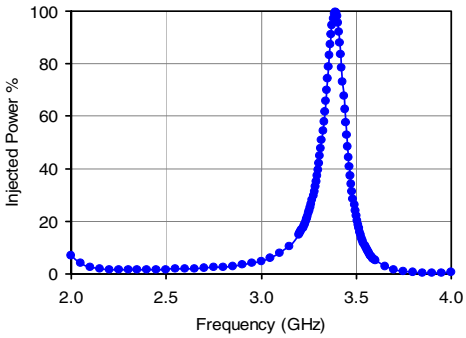

(d)

Fig. 6. (*Continued.*)

Fig. 5 shows far field calculations in the XZ-Plane (Planar Cut, phi=0).

Fig. 6 shows far field calculations in the XZ-Plane (Planar Cut, phi=0). The normalized far-field components (Elhp, Erhp, Eco, and Ecross) are normalized with respect to:

$$\max\left(\sqrt{\left|E_\theta(\theta,\phi)\right|^2+\left|E_\phi(\theta,\phi)\right|^2}\right).$$

The measured antenna gain for frequencies within the CP bandwidth is about 6.8–7.8 dBi, the measured antenna directivity within the CP bandwidth is about 7.8–8.4 dBi and the Radiated Power within the CP bandwidth is about 0.004 to 0.0018 Watts.

The radiation efficiency within the CP bandwidth is close to 80%, and remains constant in both Planar and Conical cuts.

B. 3-D Far Field Calculations at 3.4 GHz

3-D far field calculations were performed with the Finite Element Method.

Table 1. Antenna Parameters

Resonant Frequency (GHz)	3.4	
Radiated power (Watts)	0.00167	
Effective angle (Steradians)	1.78818	
Directivity (dB)	8.46798	
Gain (dB)	6.80792	
Maximum radiation intensity (Watts/Steradian)	0.00094	
Direction of maximum radiation intensity (theta, phi), (degrees)	57	0
E(theta) max (magnitude, phase)	0.83996	-134.7
E(phi) max (magnitude, phase)	0.00664	25.5
E(x) max (magnitude, phase)	0.45748	-134.7
E(y) max (magnitude, phase)	0.00664	25.5
E(z) max (magnitude, phase)	0.70445	45.3

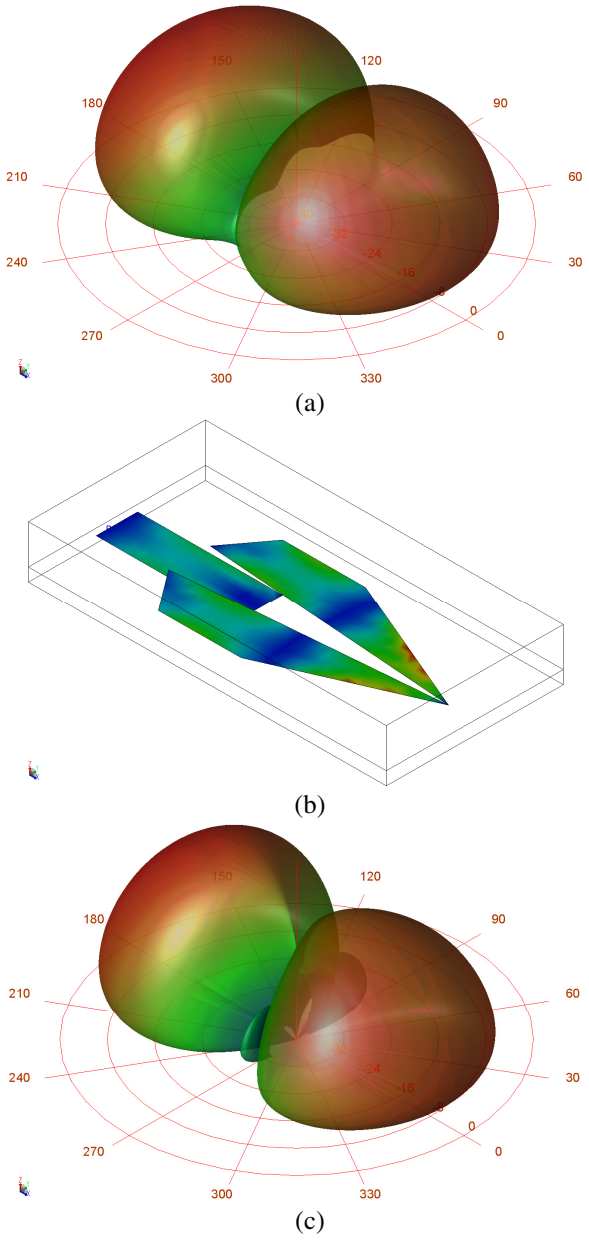

Fig. 7. (a) 3-D Normalized E, (b) Animation snapshot of the electric field in all directions, (c) Normalized ETheta and (d) Normalized EPhi, for the 3.4 GHz

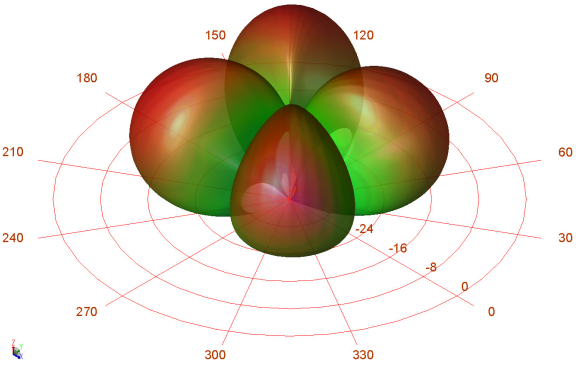

(d)

Fig. 7. (*Continued.*)

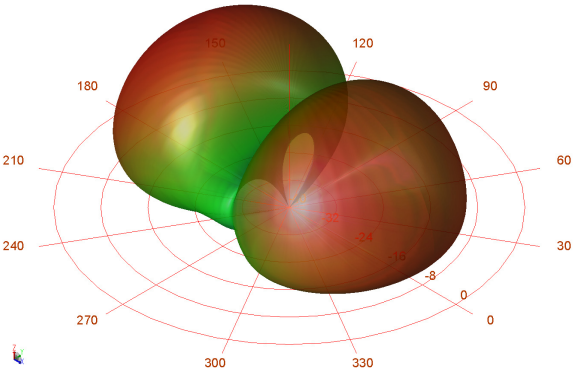

(a)

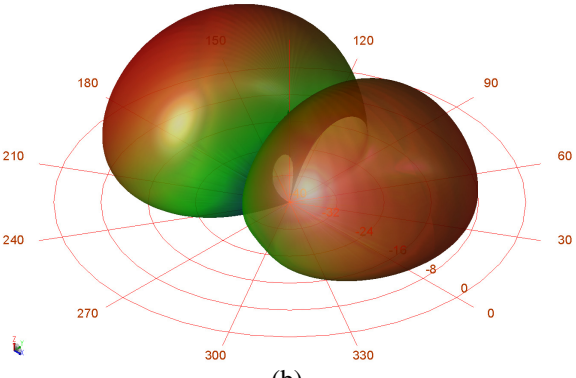

(b)

Fig. 8. 3-D Normalized **(a)** ELeft, **(b)** ERight **(c)** ECo and **(d)** ECross, for the 3.4 GHz

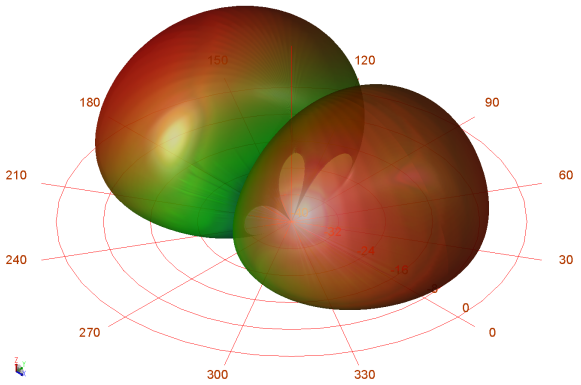

(c)

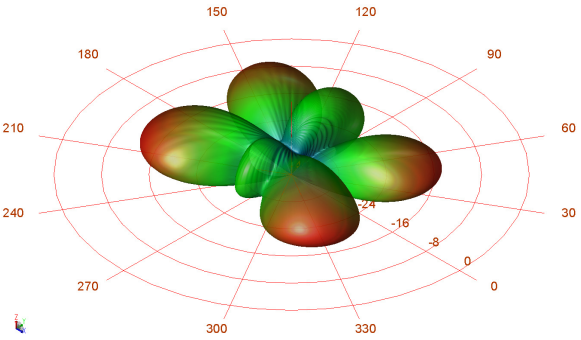

(d)

Fig. 8. (*Continued.*)

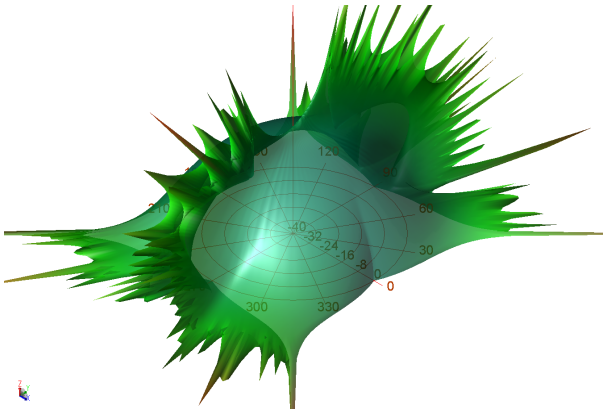

(a)

Fig. 9. 3-D Normalized **(a)** Linear Axial Ratio, **(b)** Circular Axial Ratio, for the 3.4 GHz

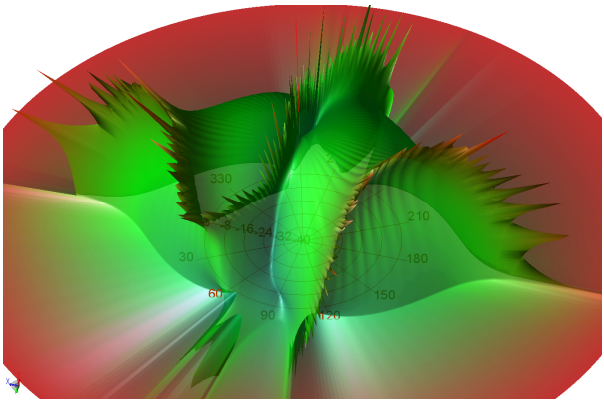

(b)

Fig. 9. (*Continued.*)

4 Conclusion

In this paper we focus on the performance of a printed antenna for WiMax (3.4 GHz) applications. It has the good characteristics of omnidirectional radiation patterns and very wide impedance bandwidth. The total volume of the antenna is 20 (L)x7.64 (W)x0.4 (H) mm^3, which is greatly reduced by 36% compared to generally internal printed radiators.

References

[1] Batra, A.: MultiBand OFDM physical layer specification. MultiBand OFDM Alliance Special Interest Group (2005)

[2] Mishra, A., Yadav, N.P., Kamakshi, Singh, A.: Analysis of pair of L-shaped slot loaded patch antenna for WLAN application. In: International Conference on Power, Control and Embedded Systems (ICPCES), pp. 1–5 (2010)

[3] Song, Y., Jiao, Y.-C., Zhao, G., Zhang, F.-S.: Multiband CPW-FED Triangle-Shaped Monopole Antenna for Wireless Applications. Progress In Electromagnetics Research, PIER 70, 329–336 (2007)

[4] Song, Z.-N., Ding, Y., Huang, K.: A compact multiband monopole antenna for WLAN/wimax applications. Progress In Electromagnetics Research Letters 23, 147–155 (2011)

[5] Zhao, Q., Gong, S.-X., Jiang, W., Yang, B., Xie, J.: Compact wide-slot tri-band antenna for WLAN/WiMAX applications. Progress In Electromagnetics Research Letters 18, 9–18 (2010)

[6] Kang, L., Yin, Y.-Z., Li, H., Huang, W.-J., Zheng, S.-F.: Dual-wideband symmetrical G-shaped slotted monopole antenna for WLAN/WiMAX applications. Progress In Electromagnetics Research Letters 17, 55–65 (2010)

[7] Chien, Y.P., Horng, T.S., Chen, W.S., Chien, H.H.: Dual wideband printed monopole antenna for WLAN/WiMAX applications. IEEE Antennas Wireless Propag. Lett. 6, 149–151 (2007)